

This article was downloaded by:

On: 14 January 2011

Access details: *Access Details: Free Access*

Publisher *Taylor & Francis*

Informa Ltd Registered in England and Wales Registered Number: 1072954 Registered office: Mortimer House, 37-41 Mortimer Street, London W1T 3JH, UK



Molecular Simulation

Publication details, including instructions for authors and subscription information:

<http://www.informaworld.com/smpp/title~content=t713644482>

OH frequency calculations for the hydroxylated MgO(001) surface

Maria Alfredsson^a; Kersti Hermansson^a

^a Department of Material Chemistry, The Ångström Laboratory, Uppsala University, Uppsala, Sweden

Online publication date: 26 October 2010

To cite this Article Alfredsson, Maria and Hermansson, Kersti(2002) 'OH frequency calculations for the hydroxylated MgO(001) surface', *Molecular Simulation*, 28: 6, 663 — 681

To link to this Article: DOI: 10.1080/08927020290030198

URL: <http://dx.doi.org/10.1080/08927020290030198>

PLEASE SCROLL DOWN FOR ARTICLE

Full terms and conditions of use: <http://www.informaworld.com/terms-and-conditions-of-access.pdf>

This article may be used for research, teaching and private study purposes. Any substantial or systematic reproduction, re-distribution, re-selling, loan or sub-licensing, systematic supply or distribution in any form to anyone is expressly forbidden.

The publisher does not give any warranty express or implied or make any representation that the contents will be complete or accurate or up to date. The accuracy of any instructions, formulae and drug doses should be independently verified with primary sources. The publisher shall not be liable for any loss, actions, claims, proceedings, demand or costs or damages whatsoever or howsoever caused arising directly or indirectly in connection with or arising out of the use of this material.

OH FREQUENCY CALCULATIONS FOR THE HYDROXYLATED MGO(001) SURFACE

MARIA ALFREDSSON[†] and KERSTI HERMANSSON

*Department of Material Chemistry, The Ångström Laboratory, Uppsala University, Box
538, SE-751 21 Uppsala, Sweden*

(Revised 1 April 2001; In final form 1 August 2001)

We have performed periodic Hartree–Fock calculations for OH groups adsorbed on the MgO(001) surface considering different surface coverages. Six types of OH groups are discussed: OH[−], OH[•], H⁺, H[−] and hydrogen-bonded OH and H. It is found that when both OH and H are present on the surface, the two groups are best described as OH[−]. We suggest that the highest-frequency fundamental band (~3750 cm^{−1} in the experimental OH spectrum) is assigned to OH[−] groups adsorbed on top of Mg²⁺, while H⁺ adsorbed on top of O^{2−} give rise to the broader band at ~3550 cm^{−1}.

Keywords: Hartree–Fock; MgO; Hydroxylated surface

INTRODUCTION

MgO is one of the simplest ceramic materials. Its {001} surface is known to be highly stable and unreconstructed. These properties make magnesium oxide a prototype system for the study of adsorption processes at oxide surfaces. Infrared (IR) spectroscopy and electron energy loss spectroscopy (EELS) have been successful in characterising adsorbed molecules on surfaces. At ambient temperature, protons are usually present on the MgO surface in the form of OH groups, formed by dissociative adsorption of water [1–4]. This interpretation is based on the fact that the characteristic water bending band at ~1600 cm^{−1}, is no longer observed in the IR spectrum of the hydroxylated MgO surface. The

[†]Current address: Davy Faraday Research Laboratory, The Royal Institution of Great Britain, 21 Albemarle Street, London W1S 4BS, UK. E-mail: mariaa@ri.ac.uk.

interpretation of the experimental IR spectrum of OH groups on MgO(001) is complicated, however. One reason is the overlap of bands from O–H groups on different phases, on different sites, with different orientations, with couplings to neighbouring OH groups, etc. as proposed by, for example, Knözinger *et al.* [1]. The purpose of the present study is to contribute to the interpretation of experimental vibrational spectra of adsorbed OH groups on the MgO surface. The IR measurements [1–4] show a sharper band at $\sim 3750\text{ cm}^{-1}$ ($\sim 50\text{ cm}^{-1}$ wide) and a broader band centred around 3550 cm^{-1} ($\sim 200\text{ cm}^{-1}$ wide), on heating the band at $\sim 3550\text{ cm}^{-1}$ decreases in intensity and vanishes at a coverage (θ) corresponding to less than 0.25 monolayers [3], while the band at $\sim 3750\text{ cm}^{-1}$ gets weaker, but sharper and is downshifted by $\sim 20\text{ cm}^{-1}$.

Theoretical investigations of OH groups and their presence on the MgO surface are presented in, for instance Refs. [5–11]. Hartree–Fock calculations [5], using a local pseudo potential to represent the crystal effect, indicate that various OH species form on the surface depending on the water coverage and number of reaction steps investigated. According to these authors, two OH species, from now on referred to as groups C and D (Fig. 1c) form in the first reaction step. Adsorption energies and geometries for the OH groups have also been presented in Refs. [6–11], where it was suggested that an OH^- ion adsorbed on top of the Mg^{2+} site is more stable than a proton adsorbed on top of the O^{2-} ion.

The importance of considering both dissociated and physisorbed water for a monolayer of water on the non-defective {001} surface of MgO are shown in recent periodic plane-wave-basis pseudopotential calculations [12–14]. It is shown in Ref. [15] that an island of three or more coupled water molecules dissociates. Harmonic vibrational frequencies determined for both a chemisorbed and physisorbed state of the water molecule on the MgO(001) non-defective surface shows that the stretching frequencies of the “free” OH bonds (corresponding to the group denoted ‘C’ in Fig. 1c) are higher than the OH

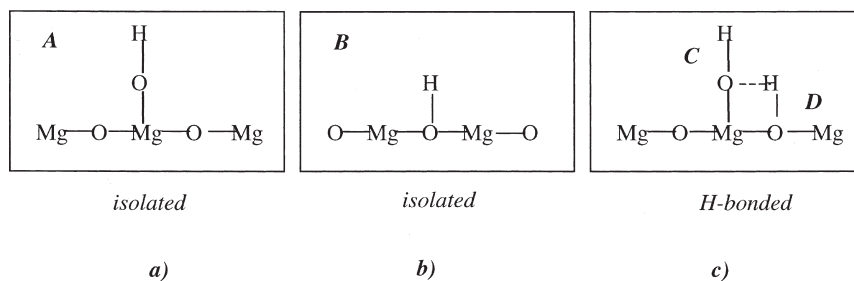
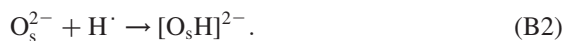
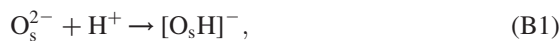
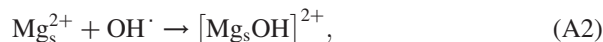


FIGURE 1 Schematic pictures of the four different types of OH groups suggested by Knözinger *et al.* [1]. The groups are denoted (a) A, (b) B and (c) C and D. When the ad-molecule is OH^- we use types A1 and B1, and for OH we use types A2 and B2.

stretching frequency of the group denoted D (Fig. 1c) in our study [14]. With reference to these findings and IR measurements by Knözinger *et al.* [1] we will here exclusively discuss the case of dissociated water.

The current paper is primarily concerned with OH vibrational frequencies, examining the properties of different OH-groups adsorbed on the MgO(001) surface. We have performed periodic Hartree–Fock calculations on the hydroxylated {001} surface of MgO, considering different surface coverages. Four types of OH groups denoted, A, B, C and D (Fig. 1) were first proposed by Andersson *et al.* [16] and later used by Knözinger *et al.* [1] in their assignment of the bands in their experimental spectra. In the present paper, we will particularly refer to the results by Knözinger *et al.* [1], who assigned the peak at 3750 cm^{-1} to the geometrically and structurally different groups A, B and C (see Fig. 1), while the broader peak at 3550 cm^{-1} was assigned to group D. In the present study, we have gone one step further and will discuss two types of group A and two types of B as defined below (where ‘s’ denotes substrate):



In this paper, we discuss the frequency shifts for OH groups A1, A2, B1, B2, C and D, adsorbed on the ideal MgO(001). We have found no previous periodic Hartree–Fock calculations concerning the vibration of OH groups on MgO surfaces. The experimental band at $\sim 3750\text{ cm}^{-1}$ corresponds to an upshift of $\sim 190\text{ cm}^{-1}$ regardless of whether we choose OH^- or OH^\cdot as the reference state, since both are about the same frequency ($\nu^{\text{free}}(\text{OH}^-) = 3556\text{ cm}^{-1}$ [17] and $\nu^{\text{free}}(\text{OH}^\cdot) = 3563\text{ cm}^{-1}$ [18,19]). The broad band centred around 3550 cm^{-1} thus corresponds to a downshift of more than 10 cm^{-1} .

METHOD

Geometries

In the model employed, we have no access to derivatives of the energies and, as a consequence, full geometry optimisations of the systems are limited. It also restricts our possibility to use more sophisticated vibrational models (where the vibrational modes are obtained from the appropriate eigenvalues). We therefore

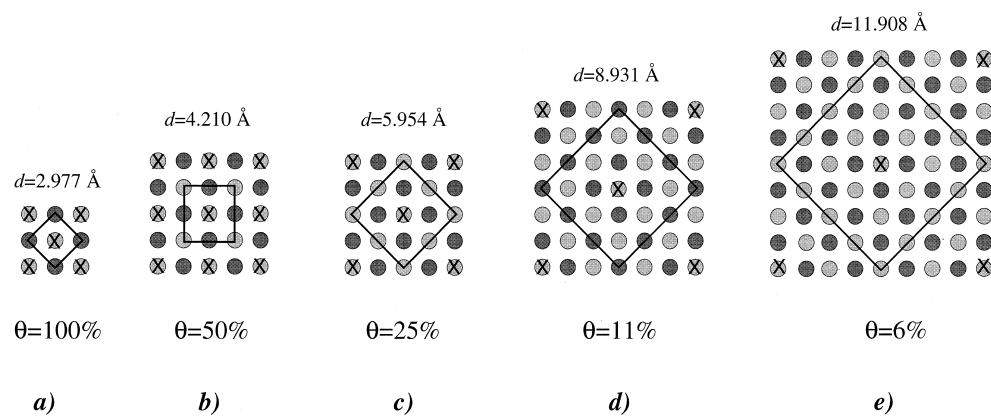


FIGURE 2 Surface coverages discussed in this work. (a) $\theta=1.00$, (b) $\theta=0.50$, (c) $\theta=0.25$, (d) $\theta=0.11$ and (e) $\theta=0.06$ monolayers. The crosses mark adsorbed molecules, while the rings mark cations and anions. d is the shortest adsorbate-adsorbate distance for each cell.

want to emphasise that the aim of the current investigation is to understand the trends of different OH-groups, and not to reproduce experimental frequencies as in Ref. [14].

For all systems investigated, the OH^- and OH groups were adsorbed in a perpendicular fashion (with the O atom down) on top of the Mg^{2+} ion on an ideal $\text{MgO}(001)$ surface, while the H^+ and H were placed above the O^{2-} ion. The slab geometry was kept fixed with a $\text{Mg}_s\text{--O}_s$ distance of 2.105 Å (the experimental value [20]), while $R(\text{Mg--O})$ and $r(\text{OH})$ for the adsorbed species were allowed to relax. Five different ordered overlayer structures have been studied: $p(1 \times 1)$; $c(2 \times 2)$; $p(2 \times 2)$; $p(3 \times 3)$; and $p(4 \times 4)$ (Fig. 2). These five surface structures correspond to surface coverages (θ) of 1.00, 0.50, 0.25, 0.11 and 0.06 monolayers, respectively.

We have constructed 1-, and 2-layer periodic slabs and small finite clusters of the MgO substrate. The clusters discussed in this paper are shown in Fig. 3; two “bare” clusters as well as the smaller Mg_6O_6 cluster embedded in 18 point charges (PC) representing the larger $\text{Mg}_{15}\text{O}_{15}$ cluster. Before adsorption of the charged or uncharged species, all clusters and the infinite slabs were neutral. The molecules were adsorbed on only one side of the slab.

Periodic Slab and Cluster Calculations

Open-shell and closed-shell restricted Hartree–Fock calculations for the infinite 1- and 2-dimensional slab were performed with the program *CRYSTAL95* (*CR95*) [21]. Cluster calculations were performed with the *GAUSSIAN94* package (*G94*)

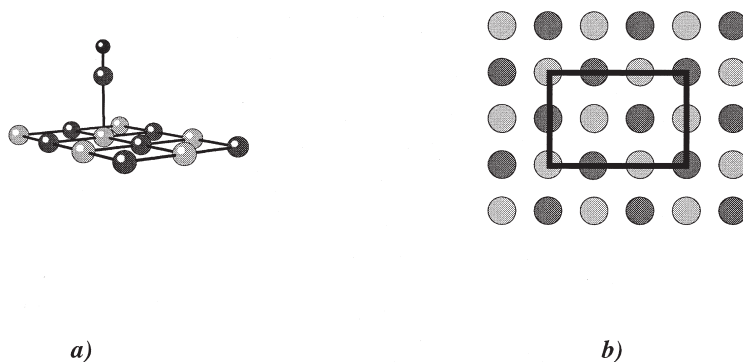


FIGURE 3 The neutral substrate clusters (a) Mg_6O_6 and (b) $\text{Mg}_{15}\text{O}_{15}$. In the $\text{Mg}_{15}\text{O}_{15}$ cluster, the Mg_6O_6 cluster is marked by a square. The atoms outside the marked square were replaced by point-charges in the embedded Mg_6O_6 cluster. The OH species in (a) is adsorbed perpendicular to the surface on top of an ion.

[22]. For all calculations, we used the 8-511G*/8-411G* [23,24] basis set for $\text{Mg}^{2+}/\text{O}^{2-}$ in the slab and the 6-31G* [25–27] basis set for O and H in the adsorbed molecules.

Cluster calculations with the *G94* program helped us determine the degree of coupling between the intra-molecular stretching vibration of an adsorbed isolated OH group and other surface modes: zero coupling was found, and we will, therefore, assume that, for low coverages the OH group vibrates as an uncoupled 1-dimensional vibrator. In *G94*, the frequencies were obtained within the harmonic approximation by diagonalisation of the force constant matrix in *G94*.

CR95 is an *ab initio* program for periodic systems in which linear combinations of Bloch functions form crystalline orbitals, where the Bloch functions are in turn combinations of Gaussian type functions, which allows us to make direct comparisons with the molecular calculations performed with *G94*. First, the $R(\text{Mg}-\text{O})$ distance was optimised by fitting a fifth-order polynomial to the potential energy curve obtained from single point calculations. To calculate the harmonic $\omega(\text{O}-\text{H})$ stretching frequency, second- and higher-order force constants were derived from the potential curve constructed from single-point energy calculations, in which the centre-of-mass (c.o.m.) of the OH molecule was kept fixed and the $R(\text{MgO})$ distance kept fixed at the optimised value obtained in step 1. A fifth-order polynomial was fitted to the potential curve:

$$V = V_0 + k_2\Delta r^2 + k_3\Delta r^3 + k_4\Delta r^4 + k_5\Delta r^5 + \dots; \Delta r = r - r_e.$$

The harmonic vibrational frequencies were obtained from:

$$\omega = \frac{1}{2\pi c} \sqrt{\frac{k_2}{m}},$$

where m is the reduced mass of OH. The $\text{O}_s\text{-H}$ group was treated in the same way, i.e. its c.o.m. was kept fixed.

In the periodic calculations, we study the in-phase stretching vibrations, since adsorbed molecules in neighbouring surface cells are necessarily identical. This means that the intramolecular stretching mode studied is actually a coupled mode where all molecules in different cells move in phase. In an earlier paper [28] we introduced the following definitions:

$$\Delta\omega_{\text{formation-of-layer}} = \omega(\text{ad-layer}) - \omega(\text{molecule}(g)),$$

$$\Delta\omega_{\text{ads-of-layer}} = \omega(\text{ad-layer/slab}) - \omega(\text{ad-layer}),$$

$$\Delta\omega_{\text{ads}} = \omega_{\text{formation-of-layer}} + \omega_{\text{ads-of-layer}},$$

where $\Delta\omega_{\text{ads}}$ corresponds to the experimentally observed stretching vibrational frequency shift.

TABLE I Harmonic frequencies calculated with *G94* for the OH^- ion and OH radical for different basis sets. The last column shows the experimental values.

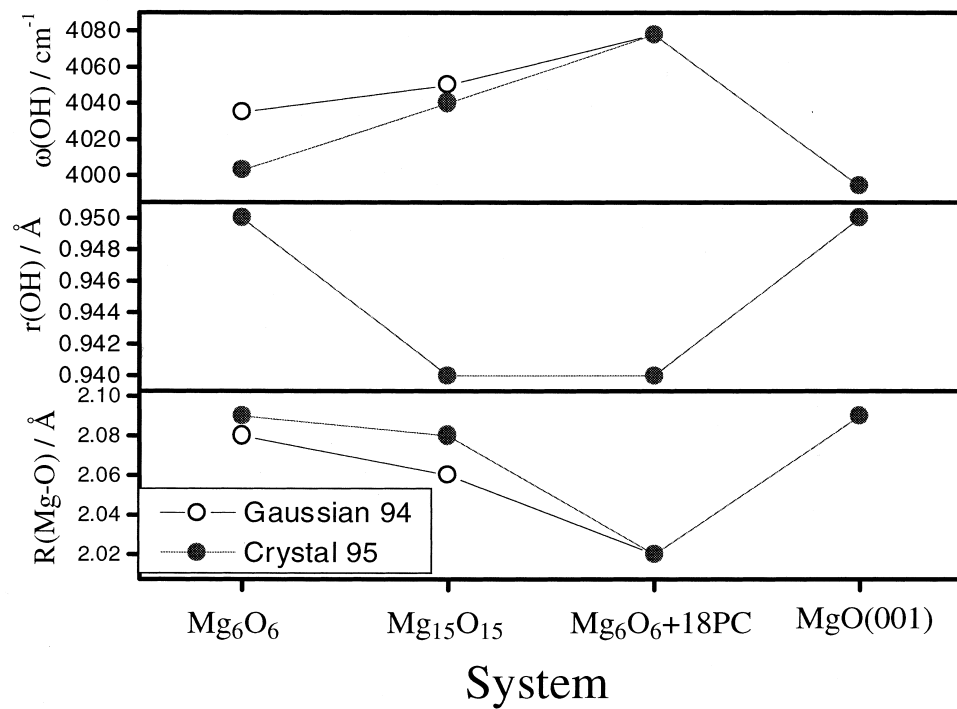
| | 6-31G* [24–27] | 6-31G** [24–27] | cc-pVTZ [29] | cc-pVQZ [29] | Extended [17] | Expt. [18,19] |
|---------------|----------------|-----------------|--------------|--------------|---------------|---------------|
| OH^- | 3739 | 3827 | 3933 | 4000 | 4068 | 3738 |
| OH | 4009 | 4156 | 4052 | 4051 | 4051 | 3739 |

In this paper, we are forced to use a rather modest basis set because of the very costly big-cluster and periodic frequency calculations involved. With the 6-31G* basis set, which we have used for the OH groups in this paper, the harmonic frequency for the OH[−] ion is much “less converged” than the OH radical frequency compared to the frequencies calculated with the extended (nearly saturated) basis set of Werner *et al.* [17] (see Table I). The extended basis set gives harmonic frequencies which are overestimated by $\sim 330\text{ cm}^{-1}$ compared to experiment due to correlation effects. It is also seen that $\omega(\text{OH}^-)$ is more sensitive to basis set effects than $\omega(\text{OH})$; the former has not yet converged to the extended-basis set value for the cc-pVQZ basis set. These results, plus the fact that we are not including correlation energy effects, make it more reasonable to discuss chemical issues in this papers in terms of frequency shifts, rather than absolute frequencies. Fortunately, harmonic OH frequency shifts for small clusters calculated at the Hartree–Fock/6-31G* level are known to well reproduce experimental frequency shifts.

RESULTS

Frequencies As a function of System Size

In the present paper, we compare frequencies obtained with small clusters to those obtained by periodic slab calculations. The harmonic vibrational frequencies for one isolated OH[−] group adsorbed on the Mg₆O₆, Mg₁₅O₁₅ and Mg₆O₆+18 point-charges (PCs) clusters (Fig. 3) have been compared with the results for a periodic 1-layer slab with $\theta = 0.06$ monolayers (Fig. 2e). Starting with the “bare” clusters it is seen in Fig. 4 that when the cluster size increases from Mg₆O₆ to Mg₁₅O₁₅ $\omega(\text{O–H})$ is upshifted by $\sim 30\text{ cm}^{-1}$, and for the periodic slab with $\theta = 0.06$ monolayers $\omega(\text{O–H})$ decreases by the same amount compared to the Mg₁₅O₁₅ value. One reason for this behaviour could be that the OH[−] groups interact with neighbouring molecules in the ad-layer. However, Table II indicates that the molecule–molecule perturbation seems almost vanished for $\theta = 0.06$ monolayers for the 1-layer slab. In Fig. 4 it is also seen that the $r(\text{OH})$ and $r(\text{Mg–O})$ distances decrease when the finite cluster size increases, while the bond lengths in the infinite system increase compared to the Mg₁₅O₁₅ cluster. The result is that the bond lengths in the Mg₆O₆ and 1-layer slab are almost the same. Ferrari and Pacchioni [30] studied the electrostatic potential (EP) at various distances from an Mg²⁺ site on the MgO surface, which was represented as clusters with different shapes and sizes as well as with periodic calculations (same code as in the present paper). For their choice of clusters, it was found that



MgO(001) SURFACE

FIGURE 4 $r(\text{OH})$, $R(\text{Mg-O})$ and $\omega(\text{OH})$ for OH^- adsorbed on Mg^{2+} (case A1) using the three clusters (Fig. 3) and the 1-layer slab with $\theta=0.06$ monolayers (Fig. 2e). Distances given in Å and ω in cm^{-1} . For computational details see the text.

TABLE II Comparison between the 1- and 2-layer substrate for the OH^- ion (case A1) or an OH radical (case A2) placed above the Mg^{2+} ion in a perpendicular fashion with respect to the molecule axis. Our computed harmonic $\omega(\text{OH})$ frequencies for the free OH^- ion and OH radical are 3709 and 3992 cm^{-1} , respectively when employing the *CR95* program.

| Coverage | Group A1 | | | | | | Group A2 | | |
|----------------|--|----------------|--|--|----------------|--|--|----------------|--|
| | 1-layer | | | 2-layer | | | 1-layer | | |
| | $R(\text{Mg}-\text{O})$ (\AA) | $r(\text{OH})$ | $\omega(\text{O}-\text{H})$ (cm^{-1}) | $R(\text{Mg}-\text{O})$ (\AA) | $r(\text{OH})$ | $\omega(\text{O}-\text{H})$ (cm^{-1}) | $R(\text{Mg}-\text{O})$ (\AA) | $r(\text{OH})$ | $\omega(\text{O}-\text{H})$ (cm^{-1}) |
| $\theta=6\%$ | 2.09 | 0.95 | 3994 | 2.13 | 0.95 | 3974 | 2.21 | 0.97 | 2994 |
| $\theta=11\%$ | 2.12 | 0.95 | 3993 | 2.14 | 0.94 | 3970 | 2.21 | 0.96 | 3581 |
| $\theta=25\%$ | 2.20 | 0.95 | 3880 | 2.21 | 0.94 | 3877 | 2.21 | 0.95 | 4046 |
| $\theta=50\%$ | 2.31 | 0.96 | 3658 | 2.32 | 0.96 | 3646 | 1.97 | 0.94 | 4210 |
| $\theta=100\%$ | 2.31 | 0.99 | 3232 | 2.32 | 0.99 | 3227 | 1.80 | 0.94 | 4329 |

the EP above their smaller neutral clusters happened to be in better agreement with the periodic slab calculation than even their largest neutral $\text{Mg}_{21}\text{O}_{21}$ cluster. Other studies (e.g. [31]) have shown that edge effects can still be important in a MgO cluster with as many as 80 atoms. This would be an explanation to the behaviour seen in Fig. 4. The small cluster, Mg_6O_6 , has also been embedded in 18 PCs with formal charges of +2 and -2, respectively, representing the larger cluster $\text{Mg}_{15}\text{O}_{15}$ (see Fig. 2b and figure caption). The OH frequency calculated for this small cluster is larger than in either of the other two clusters, demonstrating the difficulties with embedding a cluster in the “correct” environment. We conclude that it is not an easy task to model the frequencies using cluster calculations.

In Ref. [28], it was found that the vibrational frequency shifts for small polar and non-polar molecules could be correctly reproduced by a 1-layer ionic slab. OH^- , on the other hand, is a charged molecule and here we have, therefore, compared $\omega(\text{O}-\text{H})$ for the 1- and 2-layer slab. In Table II we present geometries and $\omega(\text{O}-\text{H})$ for the two substrates. We conclude that the 1-layer slab gives bond distances and frequencies in good agreement with the 2-layer slab for the OH^- ad-layers. Cases B1 and B2 are supposedly more sensitive to the modelling of the substrate thickness due to the fact that the ion is bound directly to the surface. The $r(\text{O}_s-\text{H})$ distance in the 1-layer slab was optimised to 1.02 Å, and the 2-layer slab gives the same value. The corresponding frequencies are 3152 and 3189 cm^{-1} , respectively. We therefore conclude that the 1-layer slab is also thick enough for our investigation of the adsorption of the hydroxyl ion.

Cases A1 and A2

We summarise here the main differences between the adsorption of OH^- and OH on top of the Mg^{2+} sites in MgO(001) slab. We start by describing the OH^- case (A1). When the layer is formed there are two competing factors: (i) molecule–molecule interactions within the ad-layer (repulsive); and (ii) the adsorbate–substrate interactions (attractive). It is interesting to note that as the $R(\text{Mg}-\text{O})$ distance decreases (the attractive term becomes more dominating) the intramolecular bond distance, $r(\text{OH})$, decreases as well. This is typical behaviour for the OH^- ion, but is contrary to the usual behaviour found for most molecules (including H_2O), where a stronger intermolecular bond, or substrate–adsorbate bond leads to a weakening of the intramolecular bond. This phenomenon has been discussed in the literature [32]. In the upper part of Fig. 5 and Table II it is seen that all $R(\text{Mg}-\text{O})$ distances are larger than the bulk value, but the distance decreases when the coverage decreases and it approaches the experimental bulk

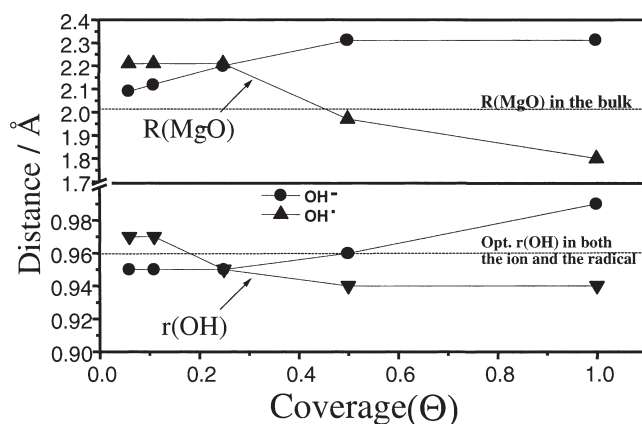
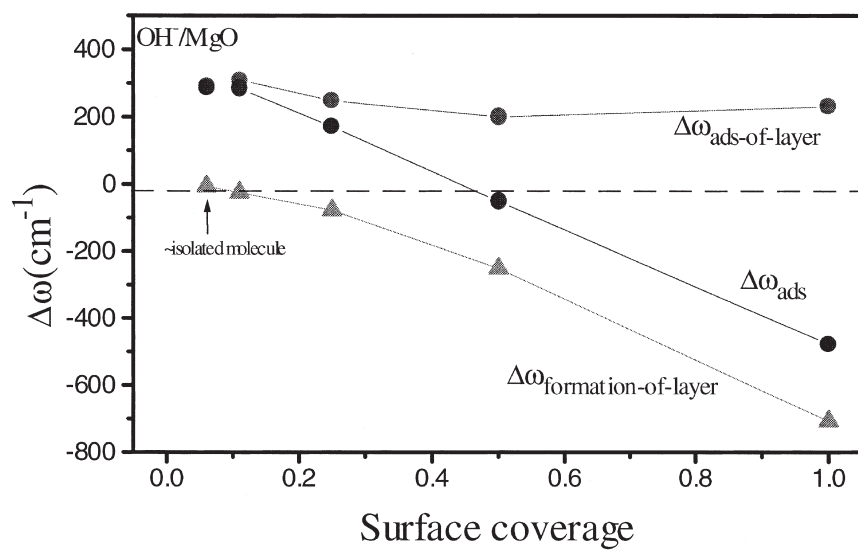


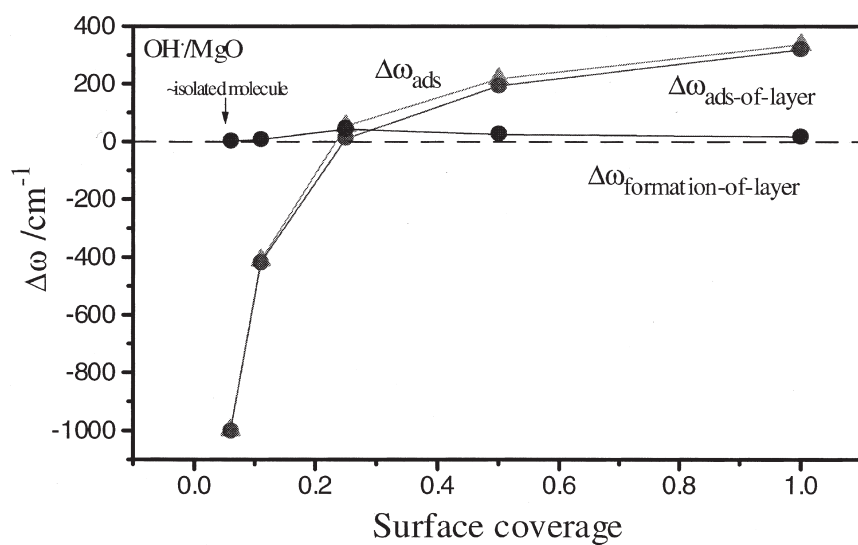
FIGURE 5 $R(\text{Mg}-\text{O})$ as a function of coverage for groups A1 and A2 are shown in the upper part of the picture. The experimental value [20] is marked. In the lower part of the picture $r(\text{OH})$ for the groups A1 and A2. The optimised $r(\text{OH})$ distance in the isolated OH^- and OH (0.96 \AA) is marked.

value, suggesting a stronger substrate–adsorbate interaction. In the lower part of Fig. 5 and Table II it is seen that the $r(\text{OH})$ distance increases when θ increases. For coverages $\theta \geq 50\%$ the $r(\text{OH})$ distance is longer than in the isolated OH^- ion indicating a weakening of the OH bond compared to the isolated ion as the ad-layer is formed. In Fig. 6a the frequency shift for the OH^- ion is shown as a function of coverage and it is seen that for coverages $\leq 25\%$ $\Delta\omega_{\text{ads}}$ for an OH^- ion adsorbed on Mg^{2+} is higher than for the isolated OH^- ion ($\omega^{\text{free}}(\text{OH}^-)=3709 \text{ cm}^{-1}$), while for larger coverages it is downshifted. The molecule–molecule and adsorbate–substrate contributions to the frequency shifts are also presented in Fig. 6a as $\Delta\omega_{\text{formation-of-layer}}$ and $\Delta\omega_{\text{ads-of-layer}}$, respectively. It is found that the $\Delta\omega_{\text{ads-of-layer}}$ term is almost constant for all coverages while $\Delta\omega_{\text{formation-of-layer}}$ shows a large variation as a function of coverage. As already mentioned, for $\theta=0.06$ monolayers the $\Delta\omega_{\text{formation-of-layer}}$ is almost equal to zero indicating no interlayer perturbation. We then conclude that for θ lower than ~ 0.40 monolayers, the dominating term is the $\Delta\omega_{\text{ads-of-layer}}$, which is the substrate–adsorbate interaction term, while for higher coverage the $\omega_{\text{formation-of-layer}}$ (adsorbate–adsorbate) interaction term dominates. The result is that $\Delta\omega_{\text{ads}}$ is upshifted for θ smaller than ~ 0.40 monolayers and downshifted for higher coverage. In Ref. [33] the frequencies of an OH^- ion in an electric field were discussed and it was found that the frequency is upshifted in the free $\text{Mg}^{2+} \cdots \text{OH}$ complex.

When the OH radical is adsorbed on the $\text{MgO}(100)$ surface (case A2) we see a different result than for the OH^- ion (see Figs. 5 and 6b). Let us start with the bond distances shown in Fig. 5. Contrary to the OH^- ion, the $R(\text{Mg}-\text{O})$ distance



a)



b)

FIGURE 6 $\Delta\omega_{\text{ads}}$, $\Delta\omega_{\text{ads-of-layer}}$ and $\Delta\omega_{\text{formation-of-layer}}$ for groups (a) A1 and (b) A2 on top of Mg^{2+} . For computational details see text.

increases for higher coverages. It is also noticeable that $R(\text{Mg}-\text{O})$ for coverages higher than $\theta=0.40$ is smaller than the bulk value. Moreover, for case A2, a shorter $R(\text{Mg}-\text{O})$ distance results in a shortening of $r(\text{OH})$ distance, i.e. $r(\text{OH})$ distance increases when the coverage decreases. A corresponding trend is also observed in the frequencies, since one almost always finds a very good (and well documented) correlation between the intramolecular bond distance and the stretching frequency (exception: see case C, below). In Fig. 6b it is seen that $\Delta\omega_{\text{ads}}(\text{OH})$ is downshifted for low coverages ($\theta \leq 11\%$) and upshifted for higher coverages. For all coverages $\Delta\omega_{\text{formation-of-layer}}$ is between 0 and 50 cm^{-1} ; this results in a negligible contribution to the $\Delta\omega_{\text{ads}}$ term, i.e. $\Delta\omega_{\text{ads}}$ is dominated by the $\Delta\omega_{\text{ads-of-layer}}$ term for all layers, which was not the case for the OH^- ad-layer.

The experimentally observed IR band centred around 3750 cm^{-1} [1] was suggested to consist of the three contributing groups A, B and C. The high frequency component ($\sim 3760\text{ cm}^{-1}$) was assigned to isolated 1-coordinated OH groups (see Fig. 1a). We thus compare this experimental band to our $\Delta\omega_{\text{ads}}$ stretching frequencies for low coverage ($\theta \leq 0.11$ monolayers). Experimentally, this band, centred at 3750 cm^{-1} , corresponds to an upshift of $\sim 190\text{ cm}^{-1}$ compared to the free OH^- ion. In Fig. 6a, it is seen that $\Delta\omega_{\text{ads}}$ for the OH^- ad-layer (case A1) in our calculations are upshifted by $\sim 300\text{ cm}^{-1}$ for coverages lower than ~ 0.25 . For $\theta \sim 0.25$ monolayers, our upshift is $\sim 200\text{ cm}^{-1}$, while for higher coverages it is downshifted. When the ad-layer is represented by OH molecules (case A2), $\Delta\omega_{\text{ads}}$ is downshifted by up to 1000 cm^{-1} for low coverages. Based on this observation, we exclude the OH molecule as a likely contributor to the experimental IR band. For coverages higher than ~ 0.30 , we also discard OH^- groups as plausible contributors to this band since $\Delta\omega_{\text{ads}}$ are all downshifted instead of upshifted compared to isolated OH^- ions, and they are, thus, better assigned to the broad peak observed at 3550 cm^{-1} . However, this case can probably also be excluded due the high repulsive interactions within the OH^- ad-layer (cf HF in Ref. [28]). When Knözinger *et al.* [1] discussed group A, they are really referring to isolated OH^- groups, and not to a situation like our $\theta = 1.00$.

Cases B1 and B2

In this section we concentrate on the group denoted B in Fig. 1b and, as for group A discussed above, two possible species are compared, namely H^+ and H defined as B1 and B2 in the Introduction, respectively. Let us start with H^+ (case B1) adsorbed on top of the O^{2-} ion on the $\text{MgO}(001)$ surface. This group gives rise to a second type of OH^- group, different from group A1 discussed earlier, because

TABLE III Distances and harmonic frequencies for H^+ (group B1) and $\text{OH}\cdots\text{H}^+$ (groups C and D) adsorbed on the $\text{MgO}(001)$ surfaces.

| Coverage | $\text{OH}\cdots\text{H}$ | | | | | | |
|----------|---------------------------|--|-------------------------|----------------|--|--------------------------|--|
| | Group B1 | | Group C | | | Group D | |
| | $r(\text{O}-\text{H})$ | $\Delta\omega$ (cm^{-1}) | $R(\text{Mg}-\text{O})$ | $r(\text{OH})$ | $\Delta\omega$ (cm^{-1}) | $R(\text{O}_s-\text{H})$ | $\Delta\omega$ (cm^{-1}) |
| 0.06 | 0.98 | -31 | 2.03 | 0.94 | 373 | 0.98 | -24 |
| 0.11 | 0.98 | -51 | 1.93 | 0.94 | 491 | 0.98 | -87 |
| 0.25 | 0.98 | -104 | 1.91 | 0.94 | 507 | 0.98 | -102 |
| 0.50 | 0.99 | -211 | 1.85 | 0.94 | 644 | 0.99 | -145 |
| 1.00 | 1.02 | -557 | 1.85 | 0.94 | 461 | 1.50 | -2415 |

of the different coordination to the surface. In Table III, $r(\text{OH})$ distances for the H^+ ion are given as a function of coverage. It is seen that as for OH^- (group A1), the $r(\text{OH})$ distance decreases as the coverage becomes lower, indicating a stronger bond. However, the $r(\text{OH})$ distances in this group are slightly longer compared to group A1, resulting in a lower absolute frequency than group A1, i.e. while group A shows an upshift compared to the free OH^- ion for low coverages group, B1 shows a downshift, as is also the case for the experimental peak at $\sim 3550\text{ cm}^{-1}$. In Table III, it is seen that the frequency becomes more downshifted as the coverages increases. At $\theta=1.00$, the downshift is $\sim 550\text{ cm}^{-1}$, suggesting that this H^+ coverage hardly exists on the hydroxylated surface and, as for group A1, we excluded high coverages due to large lateral interactions and the definition of group B. The $r(\text{OH})$ distance for the H (B2) species is longer than 1.60 \AA for all coverages discussed here, resulting in frequencies downshifted by more than 2000 cm^{-1} compared to the experimental downshift of $\sim 100\text{ cm}^{-1}$. This seems unphysical, suggesting that this group is not a possible species on the hydroxylated surface and will not be further discussed here.

Cases C and D

Until now, our discussion has concentrated on $[\text{OH}]^-$ groups not bonded to each other. Experimentally, at the initial step of the hydroxylation, higher water coverage appears and we expect groups A and B to co-exist on the surface and possibly form a hydrogen bond to each other. The resulting groups are denoted C and D (Fig. 1). In the present investigation, C and D groups are not allowed to relax completely, since they are not allowed to tilt. The result is that the $R(\text{O}\cdots\text{H})$ distance becomes too long for a hydrogen bond to form. The $\theta=1.00$ case, gives the shortest $R(\text{O}\cdots\text{H})$ distance (2.134 \AA), which is too long for a hydrogen bond.

TABLE IV Mulliken atomic and group charges for the A1, A2, B1, C and D groups when adsorbed on the MgO(001) surface.

| Coverage θ | Group A1 (OH^-) | | | Group A2 (OH) | | | Group B1 (H^+) | | | Group C (OH^-) | | | Group D (H^+) | | |
|----------------------|----------------------------|---------------|----------------|--------------------------|---------------|----------------|---------------------------|---------------|----------------|---------------------------|---------------|----------------|--------------------------|---------------|----------------|
| | $q(\text{O})$ | $q(\text{H})$ | $q(\text{OH})$ | $q(\text{O})$ | $q(\text{H})$ | $q(\text{OH})$ | $q(\text{O})$ | $q(\text{H})$ | $q(\text{OH})$ | $q(\text{O})$ | $q(\text{H})$ | $q(\text{OH})$ | $q(\text{O})$ | $q(\text{H})$ | $q(\text{OH})$ |
| 0.06 | -1.22 | +0.29 | -0.93 | -0.57 | +0.47 | -0.08 | -1.32 | +0.36 | -0.95 | -1.23 | +0.32 | -0.92 | -1.32 | +0.36 | -0.96 |
| 0.11 | -1.22 | +0.28 | -0.93 | -0.58 | +0.48 | -0.10 | -1.32 | +0.37 | -0.95 | -1.23 | +0.36 | -0.87 | -1.35 | +0.37 | - |
| 0.25 | -1.18 | +0.24 | -0.95 | -0.61 | +0.47 | -0.14 | -1.32 | +0.39 | -0.93 | -1.22 | +0.39 | -0.83 | -1.39 | +0.39 | -1.00 |
| 0.50 | -1.10 | +0.16 | -0.95 | -0.82 | +0.46 | -0.36 | -1.31 | +0.42 | -0.90 | -1.23 | +0.42 | -0.81 | -1.45 | +0.45 | -1.00 |
| 1.00 | -0.88 | -0.05 | -0.92 | -0.97 | +0.44 | -0.52 | -1.30 | +0.54 | -0.75 | -1.04 | +0.39 | -0.66 | -1.61 | +0.51 | -1.10 |

Let us start with group C and the $R(\text{Mg}-\text{O})$ distance (Table III), which we note is lengthened when the coverage decreases, opposite to the effect seen for group A1 earlier. The opposite trend is seen for the charges (Table IV): while group C becomes more negatively charged, group A1 becomes less negatively charged when the coverage decreases. For both groups, $q(\text{OH})$ converges towards $-0.90e$. The opposite trend in the $R(\text{Mg}-\text{O})$ distance is also reflected in the frequency shifts: when the coverage decreases, group C is more upshifted while group A becomes more downshifted. We notice that group A1 is less upshifted than group C and the $R(\text{Mg}-\text{O})$ distances in groups A1 and C become more similar when the coverage decreases, with the result that $\Delta\omega_{\text{ads}}$ becomes more similar. This could explain the downshift of the peak at $\sim 3750\text{ cm}^{-1}$ observed experimentally when the coverage decreases. The $r(\text{OH})$ behaviour for case C is interesting because it is constant: $r(\text{OH})$ is $\sim 0.94\text{ \AA}$ for all coverages. We note from Table III that $\omega(\text{OH})$ goes through a maximum as the coverage changes from $\theta=0.06$ to $\theta=1.00$. In these cases, the well known ω vs. r relation is no longer valid, since two branches of the ω vs. r are actually sampled as discussed in Ref. [33]. The consequence is that ω can go through rather large changes here while r remains almost constant.

The $r(\text{OH})$ in group D is almost constant (0.98 \AA) for all coverages. This is also the distance observed for group B1. However, group D is more negatively charged than group B1 and while $q(\text{OH})$ decreases for group D, $q(\text{OH})$ for group B1 increases when the coverage decreases. This means that, as for groups A1 and C, $q(\text{OH})$ for the two groups are almost the same for $\theta=0.06$ monolayers. The very similar $R(\text{Mg}-\text{O})$ distance for groups B1 and D result in an almost equal downshift for the two groups. One main difference occurs for $\theta=1.00$ where $r(\text{OH})$ is lengthened by $\sim 0.5\text{ \AA}$ for group D, but not for group B1. This unrealistic lengthening is probably a consequence of the fact that we imposed ‘perpendicular’ OH geometries. Calculations releasing this constraint are planned and will be presented elsewhere.

ASSIGNMENT AND CONCLUSION

This paper deals with the interpretation of the experimental IR spectrum for hydroxylated MgO surfaces. Two main topics are discussed: whether the proposed sites A,B, C and D contribute the observed IR bands and whether the adsorbed OH and H groups are better described as OH and H or OH^- and H^+ .

Our calculations suggest that OH and H are probably not present on the MgO(001) surface. We base our statement on the fact that our calculated frequency shifts for both OH⁻ and H resulted in downshifts of up to $\sim 2000\text{ cm}^{-1}$

with respect to the free isolated ions. To verify this conclusion, i.e. excluding the OH and H, Mulliken charges for the two groups C and D were calculated. It was found that both groups C and D come out as being OH⁻ groups at the surface (see Table IV).

Our calculated frequency shifts give that both groups A and C upshift when adsorbed on top of the Mg²⁺ ion. Experimentally, the highest band (at 3750 cm⁻¹) has been suggested to contain groups A, B and C. Our calculations support the assignment of A1 and C to the experimental band ~3750 cm⁻¹, but not B. This result is also in agreement with harmonic OH frequencies reported in Ref. [14]. We also found that the *R*(Mg–O) distance and Mulliken charges for the two groups converge towards the same value when the coverage decreases. When heating, the band splits into two peaks, Knözinger *et al.* [1] suggested the split of the band to be caused by the fact that the frequencies of groups A and B splits. We instead suggest the splitting of the band to be due to the different groups A1 and C and also suggest that C disappear before A1 on heating. This would also explain the downshift of the peak seen experimentally, since our calculations show that C becomes more downshifted when the coverages decreases.

Our calculations imply that the broad experimental peak at 3550 cm⁻¹, contains groups B1 and D, which corresponds to a proton adsorbed on the surface O²⁻ ion. Both of these groups have very similar *R*(Mg–O) distances and display similar downshifts. The Mulliken charges of these groups show an electron charge transfer from H towards O (see Table IV), which indicates that the proton is less bound than the A1 and C groups. This in turn implies a lower dissociation energy, which would explain why this peak disappears first when the hydroxylated MgO sample is heated.

One reason for the broadness of the experimental bands could be the presence of “islands” with different coverages on the surface. Another reason is the different geometries of the hydroxyl groups. To verify our results, we, therefore, need to introduce more angle flexibility in the optimisations and preferably also take different surface defects and phases into account.

Acknowledgements

This work has been supported by a grant from the Swedish National Science Research Council (NFR). Many of the calculations were performed at the National Supercomputer centre (NSC) in Linköping. Both establishments are gratefully acknowledged.

References

- [1] Knözinger, E., Jacob, K.-H., Singh, S. and Hoffmann, P. (1993), *Surf. Sci.* **290**, 388.
- [2] Coluccia, S., Lavagnino, S. and Marchese, L. (1988), *Mater. Chem. Phys.* **18**, 445.
- [3] Coluccia, S., Marchese, L., Lavagnino, S. and Anpo, M. (1987), *Spectrochim. Acta* **43A**, 1573.
- [4] Kuroda, Y., Yasugi, E., Aoi, H., Miura, K. and Morimoto, T. (1988), *J. Chem. Soc. Faraday Trans.* **84**, 2421.
- [5] Abarenkov, I.V., Tret'yak, V.M. and Tulub, A.V. (1987), *Sov. J. Chem. Phys.* **4**, 1602.
- [6] Giordano, L., Goniakowski, J. and Suzanne, J. (1998), *Phys. Rev. Lett.* **81**, 1271.
- [7] Goniakowski, J., Bouette-Russo, S. and Noguera, C. (1993), *Surf. Sci.* **284**, 315.
- [8] Langel, W. and Parinello, M. (1994), *Phys. Rev. Lett.* **73**, 504.
- [9] Langel, W. and Parinello, M. (1995), *J. Chem. Phys.* **103**, 3240.
- [10] Almeida, A.L., Martins, J.B.L., Taft, C.A., Longo, E., Andres, J. and Lic, S.K. (1998), *J. Mol. Struct. (Theochem)* **426**, 199.
- [11] Almeida, A.L., Martins, J.B.L., Taft, C.A., Longo, E. and Lester, Jr., W.A. (1998), *J. Chem. Phys.* **109**, 3671.
- [12] Odelius, M. (1999), *Phys. Rev. Lett.* **82**, 3919.
- [13] Giordano, L., Goniakowski, J. and Suzanne, J. (2000), *Phys. Rev. B* **62**, 15406.
- [14] Delle Site, L., Alavi, A. and Lynden-Bell, R.M. (2000), *J. of Chem. Phys.* **113**, 3344.
- [15] Cho, J.-H., Park, J.M. and Kim, K.S. (2000), *Phys. Rev. B* **62**, 9981.
- [16] Andersson, P.J., Horlock, R.F. and Olivier, J.F. (1965), *Trans. Faraday Soc.* **61**, 2754.
- [17] Werner, H.-J., Rosmus, P. and Reinsch, E.-A. (1983), *J. Chem. Phys.* **79**, 905.
- [18] Herzberg, G. (1950) *Molecular Spectra and Molecular Structure, I. Spectra of Diatomic Molecules* (van Nostrand Reinhold Company, New York).
- [19] Herzberg, G. (1950) *Molecular Spectra and Molecular Structure, III. Electronic Spectra and Electronic Structure of Polyatomic Molecules* (van Nostrand Reinhold Company, New York).
- [20] Deer, W.A., Howie, R.A. and Zussman, J. (1966) *An Introduction to the Rock Forming Minerals* (Longman, Harlow, Essex, UK).
- [21] Dovesi, R., Saunders, V.R., Roetti, C., Causa, M., Harrison, N.M., Orlando, R., Aprà, E. (1996), "CRYSTAL95", Theoretical Chemistry Group, University of Turin, and SERC Daresbury Laboratory.
- [22] GAUSSIAN94, Frisch, M.J., Trucks, G.W., Sclegel, H.B., Gill, P.M.W., Johnson, B.G., Robb, M.A., Cheeseman, J.R., Keith, T.A., Petersson, G.A., Montgomery, J.A., Raghavachari, K., Al-Laham, M.A., Zakrzewski, V.G., Ortiz, J.V., Foresman, J.B., Cioslowski, J., Stefanov, B.B., Nanayakkara, A., Challacombe, M., Peng, C.Y., Ayala, P.Y., Chen, W., Wong, M.W., Andres, J.L., Replogle, E.S., Gomperts, R., Martin, R.L., Fox, D.J., Binkley, J.S., Defrees, D.J., Baker, J., Stewart, J.P., Head-Gordon, M., Gonzalez, C., Pople, J.A. (1995), Gaussian Inc., Pittsburgh PA.
- [23] McCarthy, M.I. and Harrison, N.M. (1994), *Phys. Rev. B* **49**, 8574.
- [24] Harrison, N.M. and Saunders, V.R. (1992), *J. Phys.: Cond. Mat.* **4**, 3873.
- [25] Hehre, W.J., Ditchfield, R. and Pople, J.A. (1972), *J. Chem. Phys.* **56**, 2257.
- [26] Hariharan, P.C. and Pople, J.A. (1973), *Theor. Chim. Acta* **28**, 213.
- [27] Gordon, M.S. (1980), *Chem. Phys. Lett.* **76**, 163.
- [28] Hermansson, K. and Alfredsson, M. (1998), *Surf. Sci.* **411**, 23.
- [29] Dunning, Jr., T.H. (1989), *J. Chem. Phys.* **90**, 1007.
- [30] Ferrari, A.-M. and Pacchioni, G. (1996), *Int. J. Quant. Chem.* **58**, 241.
- [31] Orlando, R., Dovesi, R., Roetti, C. and Saunders, V.R. (1994), *Chem. Phys. Lett.* **228**, 225.
- [32] Hermansson, K. and Tepper, H. (1996), *Mol. Phys.* **89**, 1291.
- [33] Hermansson, K. (1993), *J. Chem. Phys.* **99**, 861.